NJC

Accepted Manuscript

This is an *Accepted Manuscript*, which has been through the Royal Society of Chemistry peer review process and has been accepted for publication.

Accepted Manuscripts are published online shortly after acceptance, before technical editing, formatting and proof reading. Using this free service, authors can make their results available to the community, in citable form, before we publish the edited article. We will replace this *Accepted Manuscript* with the edited and formatted *Advance Article* as soon as it is available.

You can find more information about *Accepted Manuscripts* in the Information for Authors.

Please note that technical editing may introduce minor changes to the text and/or graphics, which may alter content. The journal's standard Terms & Conditions and the Ethical guidelines still apply. In no event shall the Royal Society of Chemistry be held responsible for any errors or omissions in this *Accepted Manuscript* or any consequences arising from the use of any information it contains.

ROYAL SOCIETY OF CHEMISTRY

www.rsc.org/njc

Graphic Table of Contents

Rhodium complex of bis(diphenylphosphinomethyl) dopamine-coated magnetic nanoparticles as efficient and reusable catalyst for hydroformylation of olefins

Mohammed Nasiruzzaman Shaikh*[,a], M. Bououdina[b], Abiola Azeez Jimoh[a], Md. Abdul Aziz[a], Aasif Helal[a], Abbas Saeed Hakeem[a], Zain H. Yamani[a], Tae-Jeong Kim[c]

Magnetic nanoparticles(MNP) functionalized by a new bis(diphenylphosphinomethyl)dopamine (**bpd**) of type **MNP@bpd** were prepared, characterized and their reusability as catalysts were assessed by hydroformylation reaction.

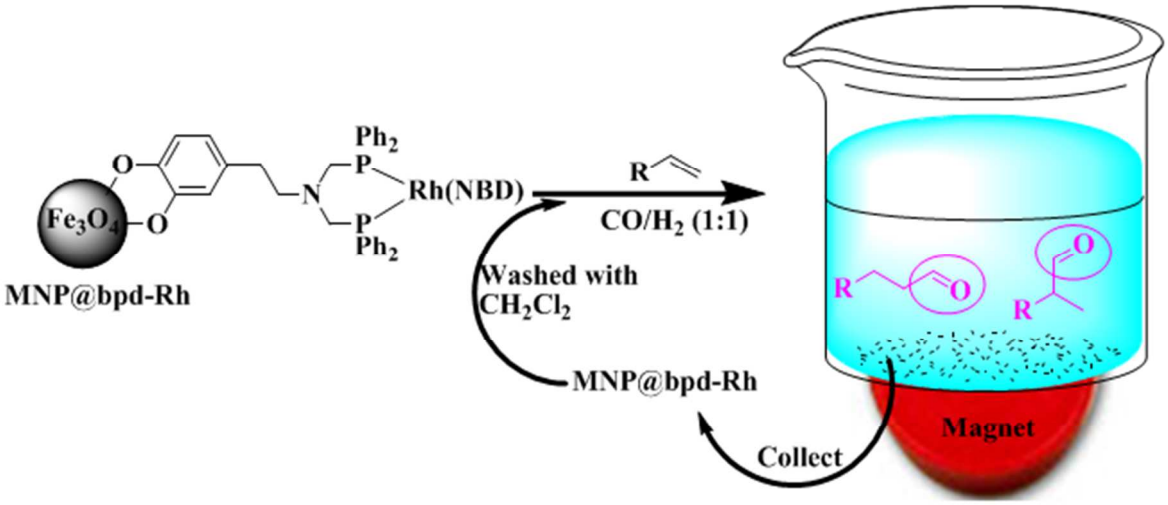

Journal Name

ARTICLE

Rhodium complex of bis(diphenylphosphinomethyl) dopamine-coated magnetic nanoparticles as efficient and reusable catalyst for hydroformylation of olefins

Received 00th January 20xx,
Accepted 00th January 20xx

DOI: 10.1039/x0xx00000x

www.rsc.org/

Mohammed Nasiruzzaman Shaikh*[,a], Mohamed Bououdina[b], Abiola Azeez Jimoh[a], Md. Abdul Aziz[a], Aasif Helal[a], Abbas Saeed Hakeem[a], Zain H. Yamani[a], Tae-Jeong Kim[c]

A new bis(diphenylphosphinomethyl) dopamine (**bpd**) ligand has been prepared and anchored on the surface of magnetic nanoparticles (MNPs). The obtained ligand and the surface functionalized nanoparticles of type **MNP@bpd** have been characterized by various analytical techniques, such as NMR, IR, TEM, XRD, and VSM. TEM shows homogeneous distribution of the particles with the size ranging 5-7 nm. XRD Rietveld analysis confirm the formation of pure and single Fe_3O_4 phase with high crystallinity. The ligands anchoring on the magnetic nanoparticles surface have been confirmed by the shift of the characteristic Fe-O vibration band in the FT-IR spectrum, and has been supported by the stepwise weight loss in TGA as a function of temperature. The phosphorus content determined by ICP-MS is approximately 0.39 mmol of phosphine per gram of the nanoparticles. Magnetization-field curves recorded at room temperature reveal superparamagnetic behavior. The materials **MNP@bpd** have proven to be an excellent catalyst after *in-situ* addition of rhodium (Rh) metal precursor for the hydroformylation reaction of styrene and its derivatives. The extent of reusability of the catalyst has been tested and was found to be active even after seven consecutive cycles.

Introduction

In recent years, catalyzed hydroformylation has drawn much attention as a commercially important reaction in the production of aldehydes from aliphatic and substituted aromatic olefins with *syngas* [1-8]. The aldehyde products can be converted into numerous useful chemicals via condensation, hydrogenation, amination and other processes. Consequently, a large number of reports on homogeneous catalysis to produce oxo- chemicals are available in the literature [9-13]. Homogeneous catalysts are dominant because they react in the same phase as the reactant. By nature, homogeneous catalysts are soluble in organic solvents, so that all catalytic sites are accessible and easy to tune by organic functional group inter-conversion. However, the solubility poses the main challenge in homogeneous catalysis; that is, to separate the catalyst from the desired product after the reaction. This limits the scope of homogeneous catalysis for some applications, and is occasionally considered as crucial drawback for product commercialization.

During the last two decades, great efforts have been devoted to develop alternatives to homogeneous catalysis in order to minimize separation costs and maximize product purity. Heterogeneous catalysis is the most obvious alternative, as it uses catalysts that are easy to separate and reuse. In addition, it can minimize the use of large quantities of environmentally toxic organic solvents that are needed for separation of the homogeneous catalysts and

[a] *Center of Research Excellence in Nanotechnology (CENT), King Fahd University of Petroleum and Minerals, Dhahran-31261, Saudi Arabia, Email:mnshaikh@kfupm.edu.sa*
[b,b] *Department of Physics, College of Science, University of Bahrain, PO Box 32038, Kingdom of Bahrain*
[c,c] *Institute of Biomedical Engineering Research, Medical School, Kyungpook National University, Buk-gu, Daegu, South Korea 702-911*

purification of the reaction products. Most heterogeneous catalysts are based on solid supports such as silica [14-16]. Silica is highly stable, robust and easy to functionalize; thereby organic functional groups can be easily anchored by either covalent binding or surface adsorption in order to provide catalytic centers. However, majority fraction of the catalytic sites can dip inside the solid support, becoming inaccessible and decreasing the overall catalytic activity. In addition, the bonds holding the catalyst to the solid support can break, causing the catalyst to leach out of the solid support and hence results in increasing the possibility of separation complications.

As an alternative support to silica, nanoparticles have attracted much attention owing to their robustness and high surface area. Because of the high surface area of nanoparticles supports, catalyst centers anchored to nanoparticles are more exposed to the reactant and therefore have increased catalytic activity. If homogeneous units are anchored onto nanoparticle supports, they can often still behave as if they were dissolved in solution, which improves the overall catalytic activity. The choice of nanoparticles can also be strategically made so that additional functionality is introduced into the catalytic system. For example, super-paramagnetic iron oxide nanoparticles (SPIONs) opened up a promising research strategy for developing surface-coated recyclable catalysts because they can easily be separated from solution using a magnetic field [17-23].

Because iron oxide nanoparticles can be prepared from low cost-materials via simple synthetic approaches, and since suitable ligands can easily be anchored on their surface [24-27], they offer excellent potential as a catalyst support. Furthermore, their insolubility in organic solvents and magnetic nature render them easily separable from the heterogeneous reaction system; this greatly reduces the efforts required to isolate the catalyst and products. In addition, it is easy to tune the physical and chemical properties, including the shape, size, and morphology, of these magnetic particles [28-30]. In line with this effort, Alper et al. recently reported magnetic particle-supported heterogeneous catalytic systems using polyaminoamido (PAMAM) dendrons, and the catalytic results obtained were encouraging [31]. They reported up to 100% conversion with excellent regio-selectivity towards branched to linear aldehyde ratio. In addition, Chouansong et al. reported the triphenylphosphine ligand coated magnetic nanoparticles with moderately high conversion of olefins [32].

Encouraged by this research, we synthesized new homogeneous species, bis(diphenylphosphinomethylated)dopamine ligands, and anchored them on magnetic nanoparticle surfaces followed by detail characterization. These particles were exploited for the conversion of a series of olefins into aldehydes, using Rh(I) as the metal centre.

Experimental

Materials and analysis

Chemicals procured from Sigma-Aldrich were used as-received unless otherwise stated. All reactions were carried out under argon atmosphere using standard Schlenk techniques. Solvents were dried using standard procedures. Deionized (DI) water was used wherever needed. The ^{1}H signatures were collected on a JEOL JNM-LA 500 Spectrometer, and the respective chemical shifts (δ) were defined using tetramethylsilane (TMS) as an internal standard. ^{31}P NMR spectra were recorded on the same machine using 85% H_3PO_4 as an internal reference. The FT-IR spectra of the functionalized MNPs were obtained from a Nicolet 720 in the range of 400 to 4000 cm^{-1}**,** using KBr. Thermal analysis was performed on the Mettler-Toledo with model TGA1 STAR^{e} System on around 10 mg of dry samples under argon atmosphere with a heating rate of 10 ^{o}C/min with the temperature ranges 0-800 ^{o}C. X-ray diffraction patterns were recorded using high resolution Rigaku Ultima IV diffractometer equipped with Cu-Kα radiation. The data were acquired over the 2θ range between 15 and 85°. Rietveld refinements were performed using PDXL program.The phosphorous content in the sample was determined by inductively coupled mass spectrometry (ICP-MS) method (Thermo Scientific, model XSERIES 2), by dissolving it in concentrated HNO_3. The surface morphology of the NPs was discerned by field emission scanning electron microscopy (FESEM, LYRA 3 Dual Beam, Tescan) operated at 30 kV. FESEM samples were prepared either from suspension or dry powder and coated with gold in an automatic gold coater for 90 s. The Energy Dispersive X-ray spectra (EDX) for the chemical and elemental analysis of NPs were collected from X-Max detector by Oxford Inc. TEM micrograph were obtained from an high-resolution transmission electron microscopy (HRTEM) (JEOL JEM-2100F) equipped with an energy dispersive X-ray spectrometer (EDX) operated at 200 kV. 300 mesh copper grids coated with carbon films were used for the imaging. The transmission electron microscopy (TEM) samples were prepared by dropping on a copper grid from an ethanolic suspension and drying at room temperature. Magnetic measurements were carried out at room temperature using PMC Micromag 3900 model Vibrating Sample Magnetometer (VSM) equipped with 1 tesla magnet and a sensitivity of 0.5 μemu. The conversion of the catalytic product were calculated by Gas chromatography (GC) (Shimadzu) and products were identified by the Gas chromatography integrated with mass-spectrometry (GC-MS) with model GCMS-QP2010 Ultra from Shimadzu.

General procedure

Synthesis of magnetic nanoparticles (MNPs). Magnetite (Fe_3O_4) nanoparticles in the range of 5-7 nm were synthesized (Scheme 1) according to the procedure reported in the literature [33-35]. Hydrated $FeCl_2$ (2 g, 10 mmol) and $FeCl_3$ (8.08 g, 20 mmol) were dissolved in 200 mL of DI water under argon at 90°C with vigorous stirring. Concentrated NH_4OH was slowly added until the solution attained a pH of 9, attended by precipitation. The mixture was

allowed to stand for 4 h. The precipitate (black color) was washed several times with DI water and dried.

Synthesis of bis(diphenylphosphinomethyl) dopamine (bpd). Dopamine was functionalized by a double phosphinomethylation step on the primary amine via the reaction of dopamine hydrochloride and diphenylphosphinomethanol, as per Scheme 1. Diphenylphosphine (1.75 mL, 10 mmol) was added to a suspension of 2.9 g paraformaldehyde (9.5 mmol) in 10 mL of anhydrous toluene under argon. The mixture was stirred for 4 h at 120°C to obtain a clear solution to which 0.76 g of dopamine hydrochloride (4 mmol) was added and refluxed for 24 h at 120°C. The resulted creamy suspension was filtered and subsequently washed first with toluene and then with chloroform and DI water to give bpd as solid with 90% yield. ^{31}P NMR (200 MHz, in DMSO-d_6): δ -28.71 (s, PPh_2) ppm. ^{1}H NMR (500 MHz, DMSO-d_6): δ 2.79 (t, 2H, NCH_2CH_2), 3.12 (t,

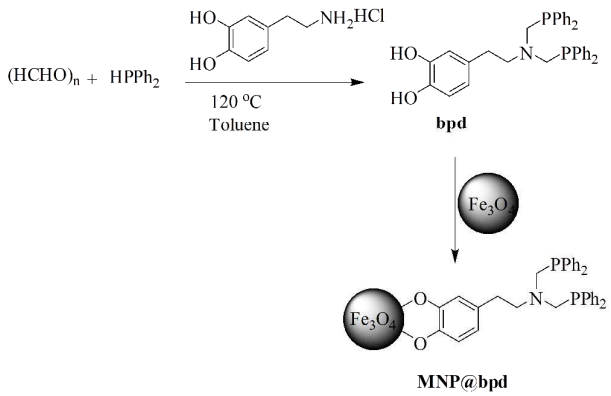

Scheme 1. Preparation of ligand (**bpd**) and **MNP@bpd**

2H, NCH_2CH_2), 4.14 (br d, 4H, CH_2P), 6.47 (d, 1H, C_6H_3), 6.55(s, 1H, C_6H_3), 6.72 (d, 1H, C_6H_3), 7.43 (br s, 12H, CH), 7.56 (br s, 8H, CH), 9.03, 9.11 (2H, OH). FT-IR in KBr (in cm^{-1}): 3124, 2926, 2571, 1628, 1436. Anal. Calcd for $C_{34}H_{33}NO_2P_2\bullet CHCl_3$: C, 62.84; H, 5.12; N, 2.09. Found: C, 62.68; H, 4.85; N, 2.32.

Synthesis of MNP@bpd. The magnetite nanoparticles (MNPs) were functionalized (Scheme 1) by modifying a reported procedure [34] as follows: 200 mg of MNPs were suspended in 10 mL anhydrous $CHCl_3$ to which a solution containing 200 mg of bis(diphenylphosphinomethyl) dopamine in anhydrous methanol was added under argon. The mixture was sonicated for 6 h. The **MNPs@bpd** were collected with the help of a strong magnet after washing repeatedly with methanol.

Catalytic hydroformylation reaction. MNP@bpd. 30 mg of **MNP@bpd** with 1 mmol of the appropriate substrate were placed in anhydrous tetrahydrofuran (THF) in a 45 mL Teflon-lined autoclave. $[Rh(NBD)Cl]_2$ (0.003 mmol, 1.3 mg) was added to this solution under argon. The sealed autoclave was purged 3 times with *syngas* (1:1 CO and H_2), pressurized at 200 psi and kept at 90°C for 16 h. After cooling to room temperature, the catalyst was magnetically separated, washed five times with dichloromethane (5 X 4 mL) and preserved for use in subsequent cycles. The products were passed through short silica gel column and injected into GC and GC-MS for identification.

Results and discussion

Synthesis: The magnetic nanoparticles were prepared by coprecipitation using Fe(II) and Fe(III) precursors in a 1:2 molar ratio. The medium of the reaction was made alkaline using concentrated ammonium hydroxide, and the pH was kept constant at 9 for 4 hours [33]. The black solid material was collected using a strong magnet after repeated washing with water to remove unreacted iron precursors. The surface of the MNPs was decorated with functionalized dopamine bound via its hydroxyl groups. The dopamine was phosphinomethylated using a straightforward reaction with a quantitative yield [35, 36]. The first step of this reaction was to prepare the phosphinoalcohol from the reaction of diphenylphosphine and paraformaldehyde in dry toluene under heating at 120°C for 4 h, until the turbid solution became clear (Scheme 1). In this reaction, equimolar amounts of dopamine hydrochloride were added *in situ* into the reaction system, which was boiled at 120°C for another 24 h. A sticky solid was precipitated and after drying under vacuum, a cream-colored solid was obtained with 90% yield. The obtained **bpd** ligand in anhydrous methanol was sonicated with the suspended solution of MNPs in chloroform for 6 h and produced a light black powder after repeated washing with methanol.

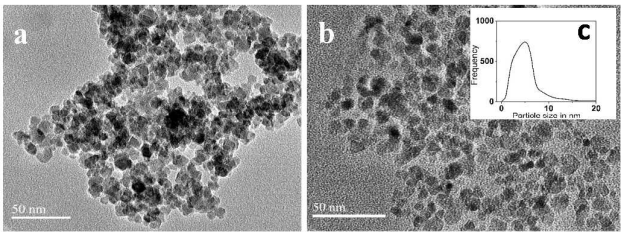

Fig. 1 TEM images of a) Fe_3O_4 and b) **Fe_3O_4@bpd** in same magnification c) particle size distribution curve

Characterization. The bis(diphenylphosphinomethylated) ligand was characterized by nuclear magnetic resonance (NMR) spectroscopy in deuterated dimethyl sulfoxide (DMSO-

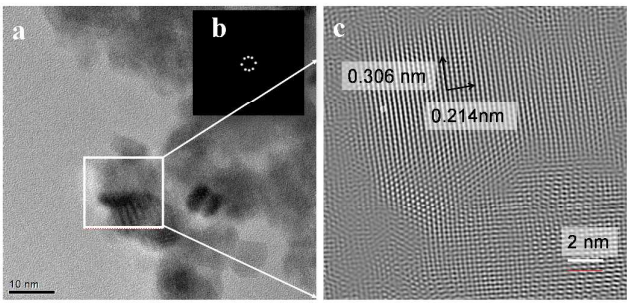

d_6).

Fig. 2 HRTEM images of a) **Fe_3O_4@bpd** b) selected area diffraction (SAED) in set c) interplaner distances are 0.306 and 0.214 nm corresponding to (220) and (400) planes.

In the ^{1}H NMR spectrum, the shift (δ) of the CH_2-P proton occurred at 4.14 ppm, and the presence of the ethylene side chain was confirmed by the alkyl proton shifts at 2.79 and 3.12 ppm. The ^{31}P NMR spectrum exhibited a shift at -28.71 ppm, which was consistent with the data in the literature [10, 37-38] (Supporting information). TEM images reveal spherical-shaped and uniformly distributed particles (Figs 1a and 1b) with average diameters between 5-7 nm. High-resolution TEM (HRTEM) images are shown in figure 2.

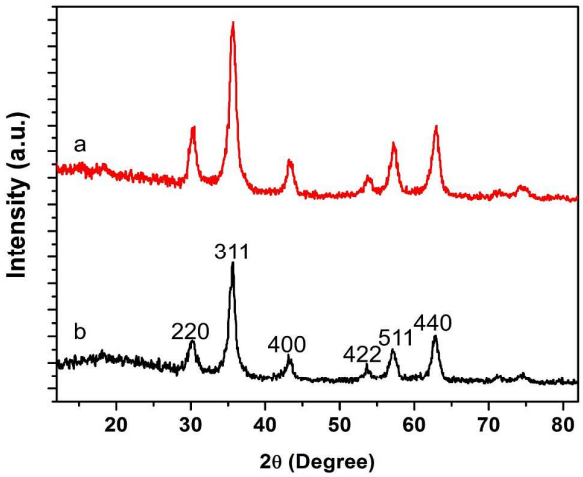

Fig. 3 XRD pattern of the a) Fe_3O_4 and b) **Fe_3O_4@bpd**

The higher order of crystallinity in the synthesized nanoparticles containing the ligand was evidenced from the Selected Area Diffraction Pattern (SADP) (Fig 2b) and the high resolution fringes (Fig 2c). The crystalline nature of the

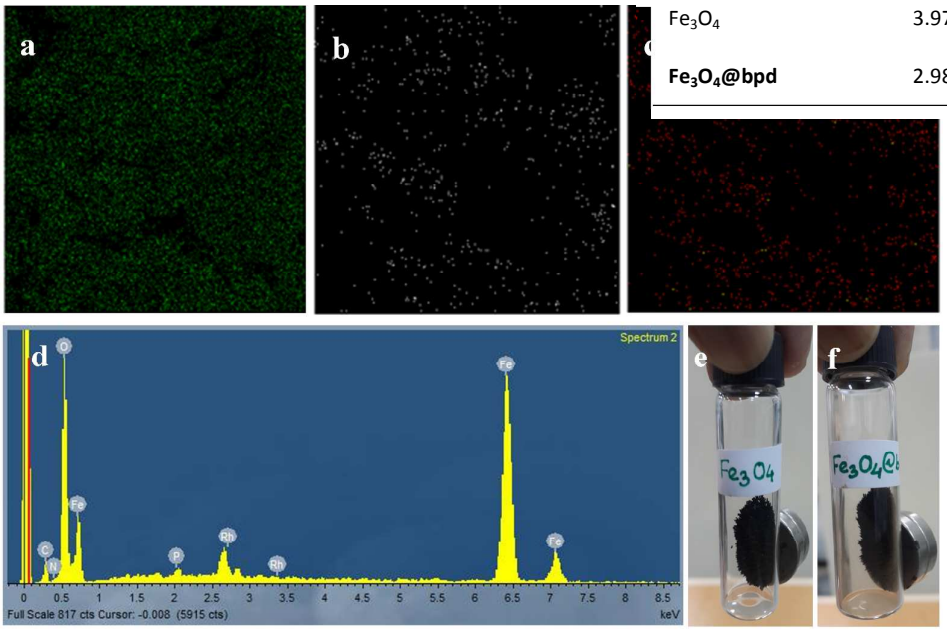

Fig. 4 Elemental mapping of a) iron b) phosphorous of and c)rhodium and d) EDX spectra of **Fe_3O_4@bpd** after the catalytic reaction and e) solid Fe_3O_4 f) solid **Fe_3O_4@bpd** in presence of magnet

MNP@bpd was further ascertained from their XRD signature (Fig. 3) The XRD peaks at 2θ=30.20°, 35.70°, 43.10°, 53.40°, 57.10° and 63.20° and the corresponding indices are marked against the peaks. All observed peaks can be indexed within cubic spinel structure, in agreement with JCPDS card No. 19-629. No additional peaks were detected thus confirming the high purity of the formed MNPs, without the presence of any other oxide or hydroxide phase(s). The broad diffraction peaks confirmed the nanocrystalline nature of the material [39-40]. Rietveld refinements of XRD patterns confirm the purity of the formed spinel cubic structure. The refined parameters are in table 1 and it can be noticed that the value of crystallite size is around 7-8 nm, in excellent agreement with the value (5-7 nm) determined from TEM observations (Supporting information) and this data is further supported by the particle size distribution data (Fig. 1**c**). However, the value of microstrain increases from 0.160% for Fe_3O_4 to 0.421% for **MNP@bpd**, which is due to the ligand surrounding Fe_3O_4. The uniform anchoring of the bpd ligand on the surface of nanoparticles were demonstrated by the Energy Dispersive *x*-ray Spectroscopy (EDX) elemental mapping shown in Fig. 4. It was revealed that the phosphorous containing ligand and their subsequent rhodium complexes obtained after the catalytic reaction were distributed homogeneously on the surface of the MNPs. However, figure 4d exhibited the EDX spectrum from the same area and marked the Rh at its designated energy levels (keV). The presence of bpd on the surface of the MNPs was further characterized by Fourier transform infrared

Sample name	H_c (Oe)	M_r (emu/g)	M_s (emu/g)
Fe_3O_4	3.97	0.802	60.17
Fe_3O_4@bpd	2.98	0.658	55.58

spectroscopy (FT-IR). The transmittance spectra of MNPs, bpd, and MNPs@bpd are shown in Fig 5. All of the characteristic peaks of the dopamine compound were observed; including the strong appearance of the Fe-O vibration shift at 593 cm^{-1} from the parent's MNPsat 587 cm^{-1}. The presence of 2933 cm^{-1} (aromatic C-H stretching), as well as the 1630 cm^{-1} and 1431 cm^{-1} bands (Fig.5c) clearly demonstrated the anchoring of the phosphinylated dopamine on the surface of MNPs. Thermal gravimetric analysis (TGA) study was conducted to investigate the thermal stability and the strong attachment of the organic ligand on the MNPs surface (Supporting information). The data showed that the weight loss at temperatures ≤ 100°C can be associated with the loss of water molecules [34]. The largest weight loss (~9%) occurred between 200 and ~450°C and could be attributed to the elimination of ligands from the surface, in few steps. The amount of bpd ligand on the surface was measured by correlation with the phosphorus content.

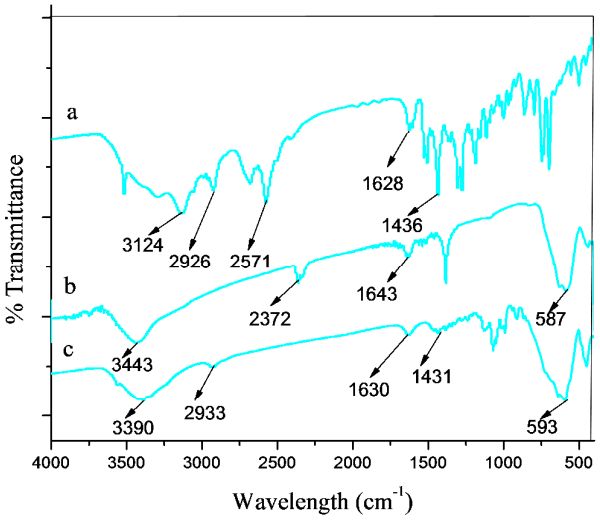

Fig. 5 FT-IR spectrum of a) **bpd** b) Fe_3O_4 c) **Fe_3O_4@bpd** with KBr pallet

The ICP data yielded approximately 0.39 mmol phosphine/g of the functionalized nanoagents. This amount of phosphine loading on the surface of magnetite was very high compared to the literature data [31, 32]. This can be attributed to the smaller size and less sterically hindered ligand and thereby occupying less area on the surface; thus, a larger number of ligands were able to bind through the phenolic oxygen to the Fe_3O_4. The possibility of leaching out of P and Rh was examined via ICP-MS measurements, the amount of **bpd** ligand remained unchanged and no Rh in the solution was traceable in early stages. This was corroborated by their ability to convert styrene completely into the corresponding formylated product in the 1st cycle. However, there was a significant (~35%) loss of from the MNP@bpd at the end of 7th cycle, due likely to successive leaching.

Magnetization-field (M-H) curves recorded at room temperature are illustrated in Fig 6. It can be clearly observed a superparamagnetic behavior for both samples. However, the presence of very small paramagnetic component (saturation cannot be reached) which was deduced using MicroMag software was observed. The magnetic parameters determined from M-H after removal of paramagnetic phase are reported in Table 1. It can noticed that the value of corecivity (H_c) is very small within the range 3.97-2.98 Oe, while the remanence (M_r) decreases slightly from 0.802 emu/g for Fe_3O_4 to 0.658 emu/g for **MNP@bpd**. Similarly to the remanence, the saturation magnetization (Ms) reduces slightly by 5 emu/g for Fe_3O_4 and **MNP@bpd**. The above changes are attributed to the attached bpd ligand on the surface of MNPs.

Table 1. Magnetic properties obtained from magnetisation-field (M-H) curves

Catalysis: The catalytic hydroformylation reaction was carried out on a series of olefins (table 2) in the presence of the *syngas* at different temperatures in a sealed autoclave pressured to 200 psi. From Table 2, it is clear that the catalyst was very active and selective toward linear aldehydes in the low temperature regime. A reversal of the selectivity was observed at high temperatures for styrene, reaching ~1.5. For example, when the catalytic reaction was run at room temperature (RT) and 50 °C for 24 hours using $RhCl_3$ as the metal precursor with styrene as the substrate in dry toluene, 35% and 100% conversion were observed with selectivities of 0.20 and 0.47 for linear and branched aldehyde, respectively. When the reaction was carried out at 120°C, the linear aldehyde (a desired product was the major product. In this reaction, a moderate amount (about 20%) of hydrogenated product was also observed, which could be attributed to the lower solubility of $RhCl_3$ in toluene. This effect can mitigate the entrance of olefins into the hydroformylation catalytic cycles. Significant changes were observed when dimeric Rh(NBD) in freshly distilled THF was used; the latter is considered as a good solvent for hydroformylation over hydrogenation because it has been reported to have led to formulation of desired products at 90°C [32].

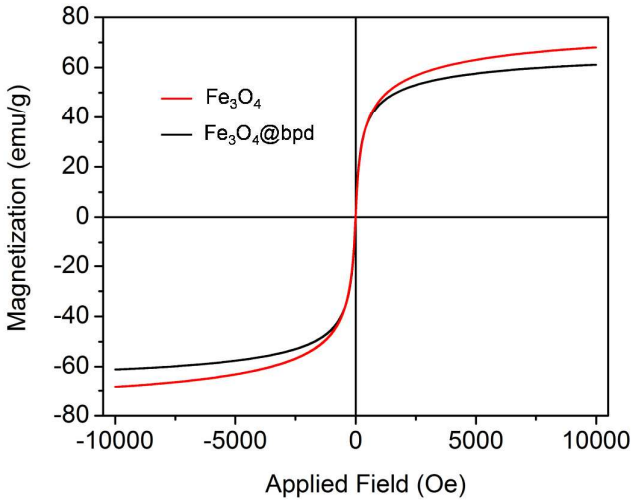

Fig. 6 Magnetic hysteresis loops of the Fe_3O_4 and **Fe_3O_4@bpd** at room temperature with 1 tesla magnet

The catalyst amount was optimized for the 1 mmol of substrate. In lower amount of catalyst (*ca* 15 mg) the 10-20 % hydrogenated product was resulted from the hydroformylation product. As the catalyst amount was increased to 30 mg, exclusively hydroformylated product was observed; these conditions (30 mg of catalyst loading and 200 psi applied pressure) are lower and hence, more benign than those reported in the literature for a similar system [31]. A series of substituted styrene were studied for the activity of the catalyst toward electron-withdrawing and electron-donating groups in different positions of the aromatic ring. However, no significant differences were observed and [26] and the result was in conformity with entries 5 and 7 in Table 2. In addition, the reactivity of 3-nitro styrene, entry 8, was found be comparatively higher in selectivity among the series at the same temperature.

Table 2. Hydroformylation[a] of olefins using **MNP@bpd** with the pressure of 200 psi using $[Rh(NBD)Cl]_2$ as metal precursor

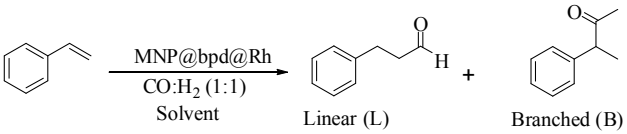

Entry	Substrate	Time (h)	Solv.	Temp (°C)	Conv[b] (%)	L	B	Ratio[c] (L:B)

1[d]	Styrene	24	Tol	RT	**35**	6	29	0.2
2[d]	Styrene	24	Tol	50	100	32	68	0.47
3[d]	Styrene	20	THF	120	100	60	40	1.50
4	Styrene	22	THF	90	100	48	52	0.92
5	4-Methylstyrene	19	THF	90	100	50	42	1.19
6	4-Vinylanisole	18	THF	90	100	46	54	0.85
7	4-Chlorosyrene	18	THF	90	100	56	44	1.27
8	3-Nitrostyrene	16	THF	90	100	57	43	1.32
9	2-Bromostyrene	24	THF	90	8	--	--	--
10	1-Octene	24	THF	90	100	49	15	3.26
11[e]	Styrene	24	THF	90	27	14	13	1.07

[a]1 mmol of styrene in 10 mL anhydrous solvent under 200 psi pressure in presence of *syn gas* ($CO:H_2$ 1:1) using 30 mg of catalyst

[b]determined by GC

[c]determined by GC-MS

[d]with $RhCl_3$

[e]in presence of MNP@bpd but without Rh metal

Surprisingly, the conversion of 2-bromostyrene was very low in same condition. This was may be due to the bigger size of the bromide adjacent to the alkene reaction site hinder olefin to coordinate with the metal to form saturated $18e^-$ species in the reaction cycle. The nanocatalysts were recycled after washing several times to remove all of the materials present after the first round of catalysis, by keeping a magnet at the bottom. The nanocatalyst was very active, even after the seven round at the same temperature, pressure and duration and it was demonstrated that with the use of 30 mg of catalyst, **MNP@bpd,** and the corresponding amount of $[Rh(NBD)Cl]_2$**,** the selectivity ratio was 0.92, and this trend existed until the second round of the reaction. However, after the 3rd rounds, the selectivity was reversed for unknown reasons. The catalyst activity was investigated towards linear olefin as well; for example, the conversion of 1-Octene, was complete (Table 2, entry #10), the linear to branched ratio, reaching a value of about 3.26. Moreover, ca. 36% of the product contained isoalkene and its hydrogenated analogue (*n*-alkane), comparable with the data reported by Sharma and Jasra [41]. For comparison, the conversion of syngas and/or styrene by Rh-free **MNP@bpd** was found to be about 27% without any selectivity towards transformation into linear-to-branch aldehyde or otherwise.

Conclusion

In conclusion, we demonstrated the synthesis of a new bis(diphenylphosphinomethyl) dopamine ligand and the anchoring of these ligand to magnetic nanoparticles through its phenolic hydroxide groups. The loading of the organic ligand on the surface of nanoparticles was found to be high. These nanomaterials exhibited high catalytic activity toward the conversion of alkenes to aldehydes; the reactions reached the maximum (100%) with a low *syngas* pressure. The recyclability was tested with the catalyst on styrene as the substrate, and it was found that even after seven cycles, without the addition of further Rh(I), the catalyst was persistently active. The material was thermally stable even at high temperatures. We believe that this new material is therefore applicable for industrial catalytic hydroformylation process, and that it may find many more applications in catalysis, a few of which are currently under study in our lab.

Acknowledgments

MNS gratefully acknowledge the National Plan for Science, Technology and Innovation (MAARIFAH)-King Abdulaziz City for Science and Technology though the Science and Technology Unit at King Fahd University of Petroleum and Minerals (KFUPM), the Kingdom of Saudi Arabia, award number 12-NAN2389-04. The authors also gratefully acknowledge the Center of Research Excellence in Nanotechnology (CENT) for providing all facilities for analysis.

References

1. R. Franke, D. Selent and Armin Börner, *Chem. Rev.,* 2012, **112**, 5675.
2. P. Eilbracht, L. Ba¨rfacker, C. Buss, C. Hollmann, B. E. Kitsos-Rzychon, C. L. Kranemann, T. Rische, R. Roggenbuck and Andreas Schmidt, *Chem. Rev.,* 1999**, 99***,* 3329.
3. C. Kubis, M. Sawall, A. Block, K. Neymeyr, R. Ludwig, A. Bçrner and D. Selent*, Chem. Eur. J.* 2014, **20**, 11921.
4. M. Kumar, R. V. Chaudhari, B. Subramaniam and T. A. Jackson, *Organometallics,* 2014, **33**, 4183.
5. C. Hou, G. Zhao, Y. Ji, Z. Niu, D. Wang and Y. Li, *Nano Research,* 2014, **7**, 1364.
6. C. Claver, P. Kalack, L. A. Oro, M. T. Pinillos and C. Tejel, *Journal of molecular Catalysis*, 1987, **43**, 1.
7. A. Orejon, C. Claver, L. A. Oro, A. Elduque and M. T. Pinillos, *Journal of Molecular Catalysis A*: Chemical 1998, **136**, 279.
8. A. B. Rivas, J. J. Pérez-Torrente, A. J. Pardey, A. M. Masdeu-Bultó, M. Diéguez and Luis A. Oro, *Journal of Molecular Catalysis A: Chemical,* 2009, **300**, 121.
9. T. T. Co and T.-J. Kim, *Chem. Commun*., 2006, 3537.
10. T. T. Co, S. C. Shim, C. S. Cho and T.-J. Kim, *Organometallics,* 2005**, 24***,* 4824.
11. V. D. M. Hoang, P. A. N. Reddy and T.-J. Kim, *Organometallics,* 2008**, 27***,* 1026.
12. T.-J. Kim, H.-Y. Lee, E.-S. Ryu, D.-K. Park, C. S. Cho, S. C. Shim and J. H. Jeong, *Journal of Organometallic Chemistry*, 2002, **649**, 258.
13. T. T. Co, S. C. Shim, C. S. Cho, D.-U. Kim and T.-J. Kim, *Bull. Korean Chem. Soc.,* 2005, **26**, 1359.
14. K. Nozaki, Y. Itoi, F. Shibahara, E. Shirakawa, T. Ohta, H. Takaya and T. Hiyama, *J. Am. Chem. Soc*., 1998, **120***,* 4051.
15. S. Ricken, P. W. Osinski, P. Eilbracht, and R. Haag*, J. Mol. Catal. A,* 2006, **257**, 78.
16. J. P. K. Reynhardt, Y. Yang, A. Sayari and H. Alper, *Adv. Synth. Catal*., 2005, **347**, 1379.
17. M. Bagherzadeh, M. M. Haghdoost and A. Shahbazirad, *Journal of Coordination Chemistry* 2012, **65**, 591.

18. H. Naeimi and S. Mohamadabadi, *Dalton Trans*., 2014, **43**, 12967.
19. N. Griffete, F. Herbst, J. Pinson, S. Ammar and C. Mangeney, *J. Am. Chem. Soc*., 2011, **133**, 1646.
20. F. Gao, H. Qu, Y. Duan, J. Wang, X. Song, T. Ji, L. Cao, G. Nie and S. Sun, *RSC Adv*., 2014, **4**, 6657.
21. S, Rana , N. V. Jadhav , K. C. Barick , B. N. Pandey and P. A. Hassan , *Dalton Trans*. 2014, **43**, 12263.
22. K. Azizi, M. Karimi, H. R. Shaterianb and A. Heydari, *RSC Adv*., 2014, **4**, 42220.
23. E. Nehlig, B. Waggeh, N. Millot, Y. Lalatonne, L. Mottea and E. Guénin, *Dalton Trans*., 2015, **44**, 501.
24. C. O. Dalaigh, S. A. Corr, Y. Gunko and S. J. Connon, *Angew. Chem. Int. Ed*., 2007, **46**, 4329.
25. F. Shi, M. K. Tse, M. M. Pohl, A. Bruckner, S. Zhang and M. Beller, *Angew. Chem. Int. Ed*., 2007, **46**, 8866.
26. N. T. S. Phan, C. S. Gill, J. V. Nguyen, Z. J. Zhang and C. W. Jones, *Angew. Chem. Int. Ed*., 2006, **45**, 2209.
27. A. H. Latham and M. E. Williams, *Acc. Chem. Res*., 2008, **41**, 411.
28. R. S. Varma, *Pure and Appl. Chem.*, 2013, **85**, 1703.
29. V. Polshettiwar and R. S. Varma, *Green Chem.*, 2010, **12**, 743.
30. V. Polshettiwar, B. Baruwati and R. S. Varma, *Chem. Commun*., 2009, 1837.
31. R. Abu-Reziq, H. Alper, D. Wang and M. L. Post, *J. Am. Chem. Soc.,* 2006, **128**, 5279.
32. C. Duanmu, L. Wu, J. Gu, X. Xu, L. Feng and Xu Gu, *Catalysis Communications,* 2014, **48**, 45.
33. K. Nezhad and S. Mohammadi, *ACS Comb. Sci.,* 2013, **15**, 512.
34. M. Koneracka, P. Kopcansky, M. Antalmk, M. Timko, C. N. Ramchand, D. Lobo, R.V. Mehta and R.V. Upadhyay, *Journal of Magnetism and Magnetic Materials,* 1999, **201**, 427.
35. J. H. Yang, B. Ramaraj and K. R. Yoon, *Journal of Alloys and Compounds,* 2014, **583**, 128.
36. R. Servin, A. Laurent, M. Romerosa, Peruzzini, J. P. Majoral and A.-M. Caminade, *Organometallics,* 2008**, 27***,* 2066.
37. O. Kuhl, S. Blaurock, J. Sieler and E. H. Hawkins, *Polyhedron,* 2001, **20**, 2171.
38. M. N. Shaikh., V. D. M. Hoang and T.-J. Kim, *Bull. Korean Chem. Soc.* 2009, **30**, 3075.
39. N. Pinna, S. Grancharov, P. Beato, P. Bonville, M. Antonietti and M. Niederberger *Chem. Mater.,* 2005, **17***,* 3044.
40. Y. Wang, B. Li, Y. Zhou and D. Jia, *Nanoscale Res Lett.,* 2009, **4**, 1041.
41. S. K. Sharma and R. V. Jasra, *Catalysis Today,* 2015, **247**, 70.